This article was downloaded by:
On: *25 January 2011*
Access details: *Access Details: Free Access*
Publisher *Taylor & Francis*
Informa Ltd Registered in England and Wales Registered Number: 1072954 Registered office: Mortimer House, 37-41 Mortimer Street, London W1T 3JH, UK

Liquid Crystals
Publication details, including instructions for authors and subscription information:
http://www.informaworld.com/smpp/title~content=t713926090

Crystal shapes of cubic mesophases in pure and mixed carboxylic acids observed by optical microscopy

M. Imperor-Clerc[a]; P. Sotta[a]; M. Veber[a]
[a] Universite Paris Sud,

Online publication date: 06 August 2010

To cite this Article Imperor-Clerc, M. , Sotta, P. and Veber, M.(2000) 'Crystal shapes of cubic mesophases in pure and mixed carboxylic acids observed by optical microscopy', Liquid Crystals, 27: 8, 1001 — 1009
To link to this Article: DOI: 10.1080/02678290050080724
URL: http://dx.doi.org/10.1080/02678290050080724

PLEASE SCROLL DOWN FOR ARTICLE

Full terms and conditions of use: http://www.informaworld.com/terms-and-conditions-of-access.pdf

This article may be used for research, teaching and private study purposes. Any substantial or systematic reproduction, re-distribution, re-selling, loan or sub-licensing, systematic supply or distribution in any form to anyone is expressly forbidden.

The publisher does not give any warranty express or implied or make any representation that the contents will be complete or accurate or up to date. The accuracy of any instructions, formulae and drug doses should be independently verified with primary sources. The publisher shall not be liable for any loss, actions, claims, proceedings, demand or costs or damages whatsoever or howsoever caused arising directly or indirectly in connection with or arising out of the use of this material.

LIQUID CRYSTALS, 2000, VOL. 27, NO. 8, 1001–1009

Crystal shapes of cubic mesophases in pure and mixed carboxylic acids observed by optical microscopy

M. IMPÉROR-CLERC, P. SOTTA and M. VEBER*

Laboratoire de Physique des Solides, Bât. 510, Université Paris Sud, 91405 Orsay Cedex, France

(*Received 10 November 1999; accepted 27 January 2000*)

Two different cubic phases in pure ($Ia\bar{3}d$ cubic space group) and mixed ($Im\bar{3}m$ cubic space group) thermotropic carboxylic acids are observed by optical microscopy. In unpolarized light, the presence of the cubic phases is identified unambiguously by the observation of facetted single crystals with highly symmetrical shapes. The observed crystal habits are growth shapes, rather than equilibrium shapes. The facetting is described, both at the interfaces with air and with the isotropic liquid phase. The facets correspond to various reticular planes that are discussed in relation with crystallographic data.

Downloaded At: 18:27 25 January 2011

1. Introduction

Lyotropic bicontinuous cubic phases, made of amphiphilic molecules and water, have been extensively studied [1–5]. They have been investigated by X-ray diffraction techniques, neutron scattering experiments and electron microscopy on freeze-fractured samples. Cubic phases are also encountered in thermotropic liquid crystals. Indeed, Gray *et al.* [6] and Kutsumizu *et al.* [7] synthesized a homologous series of 3′-nitro-4′-*n*-alkoxybiphenyl-4-carboxylic acids in which an $Ia\bar{3}d$ cubic phase was identified [8, 9]. More recently, it has been shown that increasing the aliphatic chain length induces an $Im\bar{3}m$ cubic phase [10]. The $Ia\bar{3}d$ phase is constituted by two periodic interwoven labyrinths of rods separated by a surface where the molten paraffinic chain extremities are located [11], as is the case in the inverted $Ia\bar{3}d$ phase of lyotropic systems. The rods are made of the rigid cores of the molecules.

The molecular organization in the $Im\bar{3}m$ phase is more puzzling. Recently a model with three disconnected surfaces for the paraffinic chains extremities has been proposed by Levelut and Clerc [9]. Such a complex structure is needed in order to take into account the quite large value of the cubic lattice parameter in comparison with the molecular dimensions.

The importance of optical microscopy observations in the identification of various liquid crystalline phases was recognised long ago, specifically using polarized light. Cubic phases are isotropic and therefore do not present birefringent textures. However, it has been emphasized that the three-dimensional long range order in these phases may give rise to specific crystal morphologies, as is the case, for example, for Blue phases [12]. In 1991, Sotta described the facetting of air bubbles, embedded in the lyotropic cubic phase ($Ia\bar{3}d$) of a $C_{12}EO_6$/water mixture [13]. It was shown that the facets of these 'negative crystals' corresponded to the {2 1 1} reticular planes. Also, it has been shown recently that small cubic drops of this system exhibit a devil's staircase-type facetting [14].

In this paper, we show that it is possible to grow macroscopic single crystals of two different thermotropic cubic phases. We describe facetted single crystals of cubic phases observed by optical microscopy without crossing the analyser and polarizer. We discuss the relationship between the facets of the crystals and the most dense reticular planes of their cubic space groups.

2. Experimental

2.1. *Synthesis of the molecules*

The observations were made on pure compound **1** and on a mixture of compounds **1** and **2**.

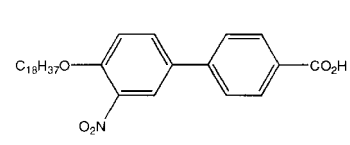

1

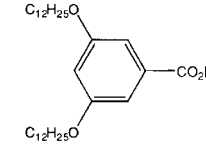

2

Compound **1** (3′-nitro-4′-*n*-octadecyloxybiphenyl-4-carboxylic acid) was prepared according to Gray's procedure [6, 15]. Compound **2** (3,5-didodecyloxybenzoic

*Author for correspondence; e-mail: veber@lps.u-psud.fr

acid) was prepared by a Williamson etherification reaction in dimethylformamide on methyl 3,5-dihydroxybenzoate using dodecyl bromide as the alkylating agent and potassium carbonate as the base [16]. The saponification of the methyl ester was carried out using alcoholic potassium hydroxide, followed by acidification of the potassium salt.

The mixture studied was prepared by dissolving the appropriate amounts of compounds **1** and **2** (molar concentration of compound **2**: 33%) in dichloromethane at room temperature. The solvent was then evaporated under reduced pressure.

2.2. *Microscopic observations*

The microscopic observations were made using a Leitz Orthoplan microscope equipped with a Mettler FP52 hot stage and FP5 central processor, and working in transmission using white, unpolarized light. The pure compound **1** or the mixture (in the crystalline state) was simply deposited on glass plates at room temperature, and then heated to the liquid isotropic phase in order to obtain small free drops. The drops wet the glass plates and spread on the surface. In some cases, the glass plates were treated to make them hydrophobic with DMOAP (dimethyl-*n*-octadecyl(3-trimethoxy silylpropyl)-ammonium chloride) [17], in order to reduce wetting and to obtain nearly spherical drops. Some observations were also made with samples mounted between glass plates. Mesophase sequences were observed with very slow heating or cooling rates (typically 0.2°C min^{-1}).

Downloaded At: 18:27 25 January 2011

2.3. *X-ray experiments*

Experiments were performed using a rotating anode generator. The copper K_α wavelength (0.1542 nm) was selected with a graphite monochromator, and a collimator gave a nearly parallel beam of 1 mm × 1 mm section at the sample position. Diffraction patterns were recorded on an image-plate detector (sample–detector distance: 46 cm ± 0.1 cm).

The mixtures were introduced into Lindemann capillaries (diameter 1 mm) which were then sealed at both ends. Capillaries were held inside an oven specifically designed to obtain large monodomains. This oven allows very slow heating or cooling rates (typically 0.01°C min^{-1}), with a controlled temperature gradient along the capillary axis. A computer controlled rotation of the capillary around its axis allows investigation of the whole of reciprocal space of monodomains obtained.

3. Results

3.1. *Phase sequences*

The phase sequence of the pure compound **1** is well known [8, 9]. It exhibits an $Ia\bar{3}d$ cubic phase (lattice parameter $a = 11.2$ nm) between a smectic C phase (layer thickness $d = 4.5$ nm) and the isotropic phase. The transition temperatures are given below:

$$\mathrm{Cr} \rightarrow \mathrm{SmC}\ (125°\mathrm{C}) \rightarrow Ia\bar{3}d\ (156°\mathrm{C}) \rightarrow \mathrm{I}\ (197°\mathrm{C})$$

Pure compound **2** is only crystalline and melts at 67°C. Various mesophases are obtained by mixing both compounds. In figure 1 is presented the phase diagram for mixtures of compound **1** and the undecyl homologue of compound **2** [18] over a wide composition range. The dashed line in the diagram indicates the concentration corresponding to the mixture used by us. We have verified by optical microscopy that the mixture studied here presents exactly the same phase sequence as that shown in figure 1, with the same transition temperatures:

$$\mathrm{Cr} + \mathrm{I} \rightarrow \mathrm{Cr} + Im\bar{3}m\ (121°\mathrm{C}) \rightarrow Im\bar{3}m\ (122°\mathrm{C})$$

$$\rightarrow Im\bar{3}m + \mathrm{I}\ (151°\mathrm{C}) \rightarrow \mathrm{I}\ (172°\mathrm{C})$$

The $Ia\bar{3}d$ cubic phase exhibited by the pure biphenyl carboxylic acid [9] persists below 5% of compound **2**. Then, by adding more substituted benzoic acid, an $Im\bar{3}m$ phase is induced. Two regions are remarkable. Between 5 and 25%, by cooling the mixture from the isotropic phase, a biphasic region of isotropic liquid and cubic $Ia\bar{3}d$ phase is observed. By further cooling, two cubic phases of different symmetries exist ($Im\bar{3}m$ and $Ia\bar{3}d$). Then, by further cooling, the $Im\bar{3}m$ phase appears in coexistence with the SmC phase. Above 25% of benzoic acid **2** (studied mixture), the $Ia\bar{3}d$ phase disappears. The $Im\bar{3}m$ cubic phase exists either in equilibrium with the isotropic liquid or the pure state, depending on the temperature and on the relative concentrations of both compounds.

The symmetry of the cubic phase obtained in the mixture was checked by X-ray diffraction using a monocrystal grown at 150°C by slow cooling (0.02 C min^{-1}) from the isotropic liquid phase (175°C). A number of well separated Bragg peaks are observed during the rotation of the sample around its axis. They may all be indexed by an $Im\bar{3}m$ cubic space group with a lattice parameter $a = 17$ nm (see the table). Figure 2 shows a pattern of the cubic phase obtained by oscillating around a particular angular position (angular sector of 15°). All the observed Bragg peaks can be indexed assuming that the oscillation is made in the vicinity of a $(0\,2\,\bar{4})$ plane of the reciprocal space, with the $[1\,\bar{2}\,\bar{1}]$ direction along the rotation axis.

3.2. *The $Ia\bar{3}d$ cubic phase in the pure compound **1***

The observations are made by slowly cooling a large free drop (diameter ≈ 0.5 mm) deposited on *an untreated glass plate* from the isotropic phase. The free surface (air/cubic interface) of the compound is observed

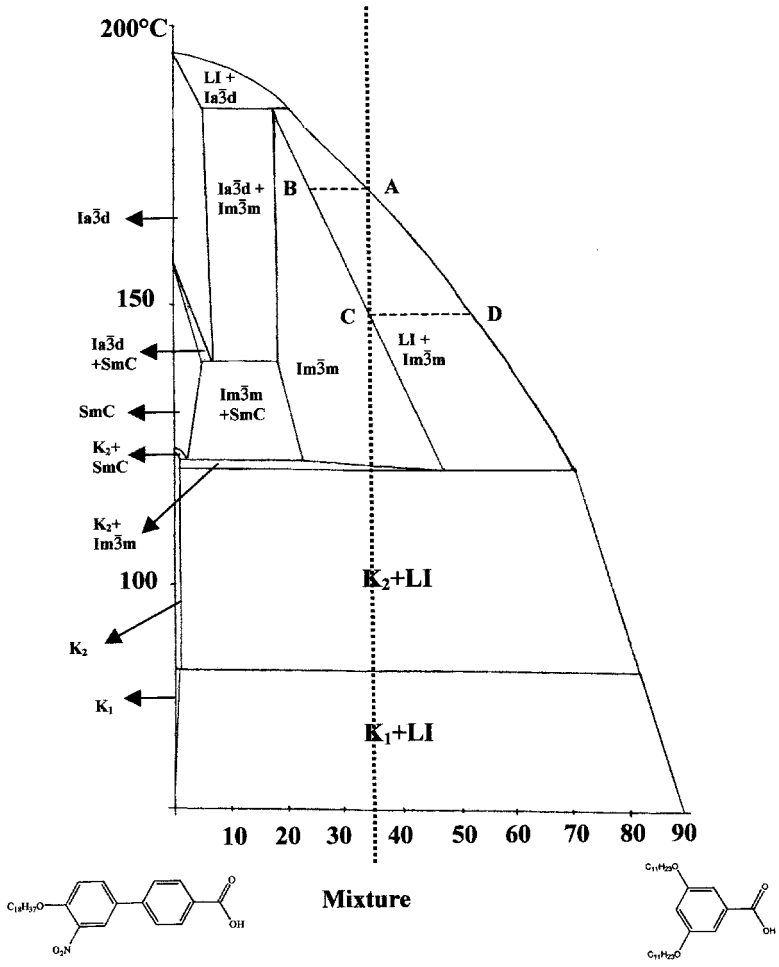

Figure 1. Phase diagram from [18] of mixtures of compound **1** and the $n = 11$ homologue of compound **2**. In this figure, K means crystalline and LI is isotropic liquid. The dashed line corresponds to the mixture studied here.

here. We observe that the periphery of the drop shows rectilinear edges and corners with an angle 109.5°, which is characteristic of (2 2 0) planes, figure 3(*a*). This suggests that a 2-fold axis is roughly perpendicular to the glass surface in this region of the drop and that a {2 2 0} face is parallel to the plate. A surface instability is observed at the upper, free surface of the drop. Starting from a macroscopically smooth curved surface, one observes (at a fixed temperature) the nucleation of small pyramids, figure 3(*b*). All nuclei have the same orientation, which shows that a single crystal occupies the whole observed field ($50 \times 40\,\mu m^2$). The angle at the summit of the pyramids is 70.5°, the complementary of 109.5°, which is obtained also by intersecting (2 2 0) planes. Then, the surface evolves into a completely developed staircase-like pattern, with macroscopic steps, figure 3(*c*). On the different plates shown, the original surface is at different angles with respect to the final facets (steps and edges), which accounts for the different aspects of the reconstructed surface, figure 3(*d*). In most cases, a 3-fold axis is roughly perpendicular to the average surface. Thus, the pattern may be constructed with {2 2 0} faces. Note that in some cases, the pattern may also be constructed with {4 0 0} faces, see figure 3(*d*), but not with {2 1 1} faces, because some angles in figures 3(*c*) and 3(*d*) are too small.

In another series of observations, we deposited the pure compound **1** on *a glass surface treated to be hydrophobic* with DMOAP, in order to observe nearly spherical droplets of constant volume (apparent diameter $\Phi \approx 50\,\mu m$).

The system was first heated to the isotropic phase in order to obtain nearly spherical droplets, then cooled into the smectic C phase, and then heated slowly step by step. The smectic layers lay roughly parallel to the plate. The purpose of heating from the SmC phase was to obtain eventually a cubic crystal with a well defined orientation. The cubic phase nucleates within the SmC phase, with the (2 2 0) planes parallel to the plate. Figure 4(*a*) shows a single crystal with a 2-fold axis perpendicular to the surface. The (2 2 0) planes form a system of terraces with a diamond-shaped contour, cut in some places by (4 0 0) planes. The same system of terraces appears in figure 4(*b*).

Downloaded At: 18:27 25 January 2011

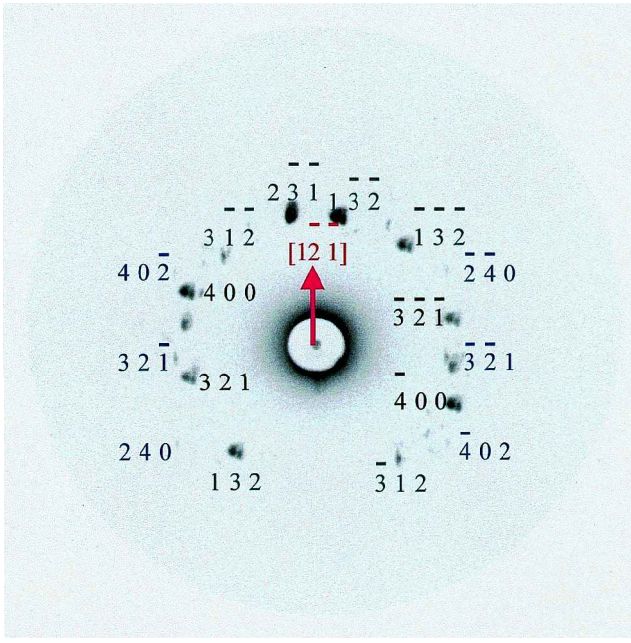

Figure 2. X-ray pattern of a single crystal of the $Im\bar{3}m$ cubic phase of the mixture at 150°C. Bragg peaks of the same colour are located in the same reciprocal plane.

Table. Observed Bragg reflections in the $Ia\bar{3}d$ and $Im\bar{3}m$ cubic phases. Some reflections permitted in the $Im\bar{3}m$ phase are not observed in the $Ia\bar{3}d$ phase. Reflections are placed in lines with similar d_{hkl} values.

Compound **1**		Mixture	
$Ia\bar{3}d$ (a = 11.2 nm)	d_{hkl}/nm (intensity[a])	$Im\bar{3}m$ (a = 17 nm)	d_{hkl}/nm (intensity[a])
		110	12.02 (-)
		200	8.5 (-)
		211	6.94 (vw)
		220	6.01 (-)
		310	5.38 (w)
		222	4.91 (w)
211	4.57 (vs)	321	4.54 (vs)
		400	4.25 (m)
220	3.96 (s)	411, 330	4.01 (s)
		420	3.80 (w)
		332	3.62 (w)
		422	3.47 (w)
321	2.99 (w)		
400	2.80 (w)		
420	2.50 (w)		
332	2.39 (w)		
422	2.29 (w)		

[a] vs: very strong; s: strong; m: medium; w: weak; vw: very weak; -: not observed.

3.3. *The $Im\bar{3}m$ cubic phase in the mixture*

3.3.1. *Observation between non-treated glass plates*

Samples prepared between glass plates are cooled very slowly from the liquid isotropic phase (LI) into the biphasic region LI + $Im\bar{3}m$ (see the phase diagram and notation in figure 1). The situation here is entirely different from the point of view of surface properties. We observe here interfaces between the isotropic phase and cubic germs embedded in it. Single crystals with various shapes nucleate. They are entirely facetted and show polyhedral habits made of plane facets delimited by edges and vertices. Figure 5 (*a*) shows a diamond-shaped single crystal with an angle at the vertex of 109.5°. This shape may be constructed with {1 1 0} faces

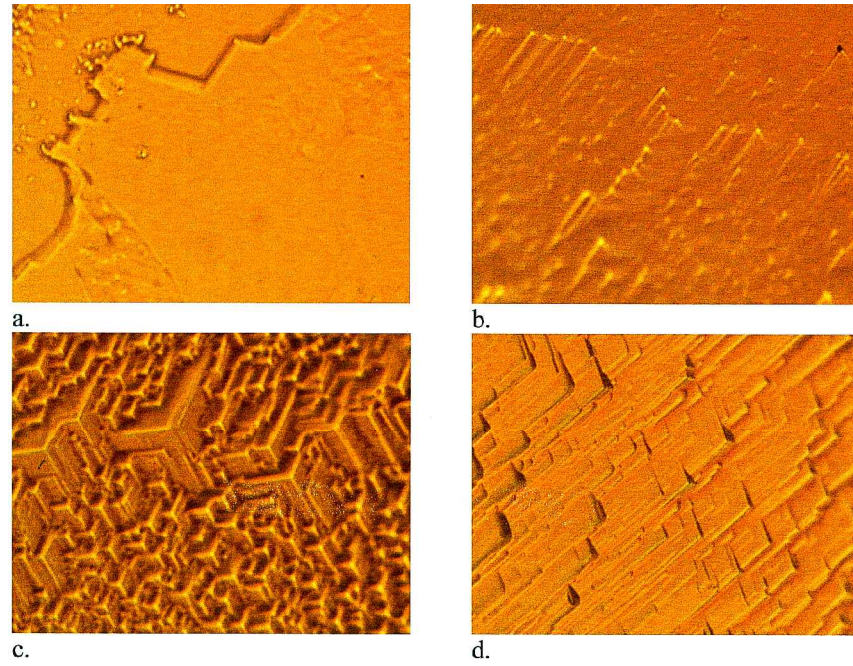

Figure 3. Facetting of the surface of a drop of pure compound **1** in the $Ia\bar{3}d$ cubic phase. The observation field covers $50 \times 40\ \mu m^2$. (*a*) Periphery of the drop; (*b*) nucleation of small pyramids with an angle of 70.5° at the beginning of the facetting process; (*c*) final reconstruction of the surface with well-developed facets—a three-fold axis is roughly perpendicular to the surface; (*d*) final reconstruction of the surface showing another orientation of the facets.

Downloaded At: 18:27 25 January 2011

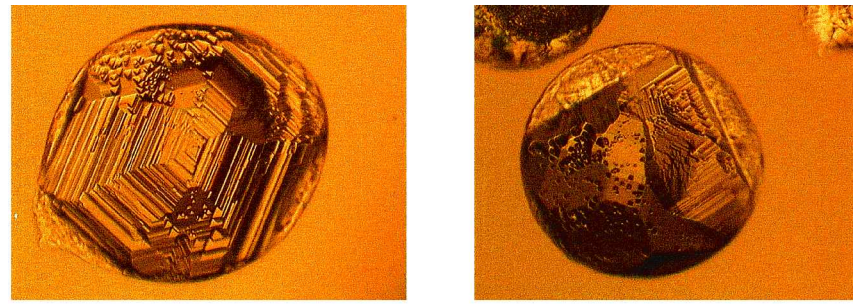

Figure 4. Droplets of pure compound **1** obtained on a treated (hydrophobic) surface. (*a*) Facetted single crystal of the *Ia*3*d* phase; (*b*) facetted single crystal of the *Ia*3*d* phase in coexistence with smectic C phase.

only, figure 5 (*c*). Note that one vertex of the crystal is truncated by a small {2 0 0} facet. Figure 5 (*b*) shows another single crystal with {2 2 2} and {2 0 0} faces, figure 5 (*d*). Figure 5 (*e*) shows a single crystal with squared faces. This shape may be constructed, either with (2 0 0) planes only, or by combining (2 0 0) and (1 0 0) planes.

Germs with a squared contour as shown in figure 5 (*e*) are quite common. This may indicate that (2 0 0) planes are preferentially anchored parallel to the glass surfaces. The observed crystal shapes are clearly not at equilibrium. They are governed by growth properties. Indeed, different growth regimes are observed: in some parts of the same

Downloaded At: 18:27 25 January 2011

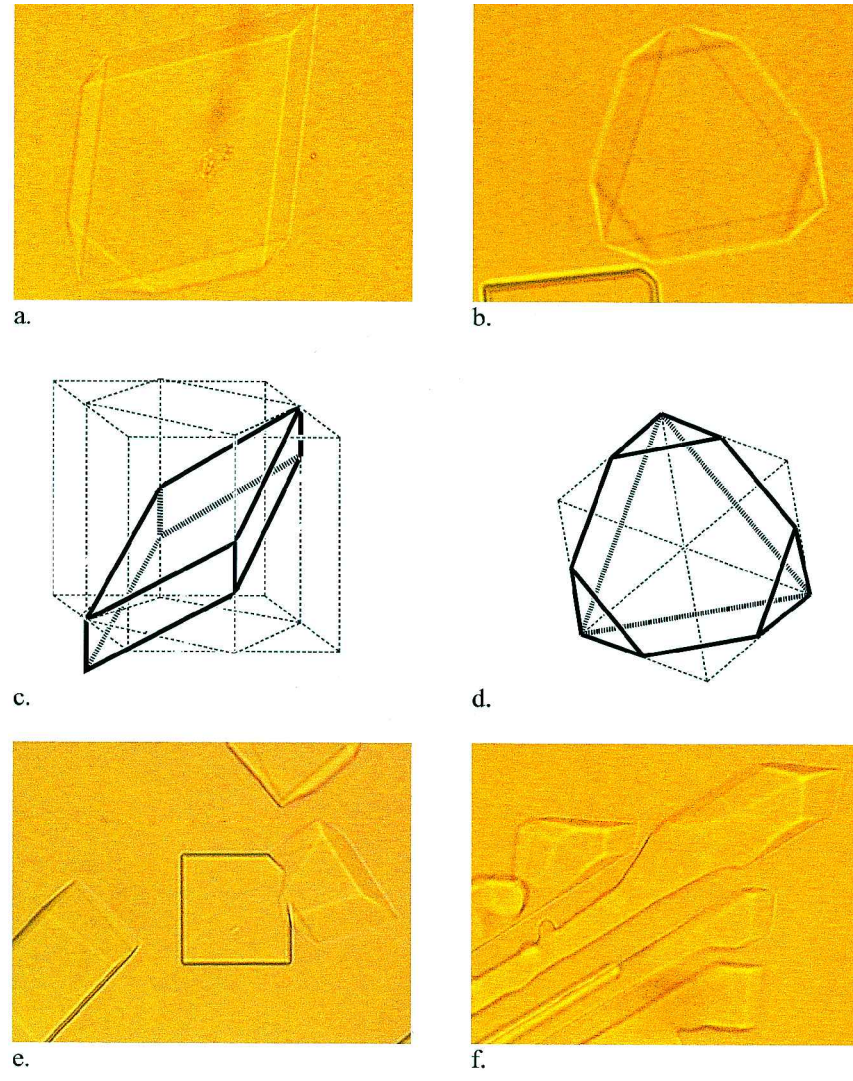

Figure 5. Coexistence of the isotropic phase and the *Im*$\bar{3}$*m* cubic phase in the mixture observed between untreated glass plates. (*a*) (*b*), (*e*) Single crystals with different morphologies; (*c*), (*d*) the constructions corresponding to (*a*) and (*b*), respectively; (*f*) facetted dendrites.

sample, the growing process is dendritic, figure 5 (*f*). A detailed analysis of dendritic growth phenomena is not the purpose of this paper. However, the shape of the dendritic germs indicates that they are growing preferentially along the [1 1 0] or the [1 0 0] directions. The coexistence of different growth regimes in the same preparation may be related to the existence of small temperature gradients: growing rates can be very different at different temperatures, i.e. at different supercooling rates. Moreover, the observations have been made by cooling the sample continuously inside the biphasic region, so that cubic germs may appear at different temperatures with quite different concentrations (segment BC in figure 1), while the isotropic liquid phase becomes more concentrated in compound **2** (segment AD in figure 1).

3.3.2. *A free drop deposited on an untreated glass plate*

A large free drop is deposited on an untreated glass plate, heated to the isotropic phase and then cooled slowly. Inclusions nucleate within the biphasic region. The inclusions evolve from quasi-spherical shapes, figure 6 (*a*), towards highly symmetric, almost completely facetted polyhedra, figures 6 (*b*) and 6 (*c*), on a time scale of a few hours. All the facetted inclusions have the same shape. In particular, inclusions of different size are homothetic, figure 6 (*c*). The observed shape corresponds to a rhombic dodecahedron, constructed with {1 1 0} faces. In figure 6 (*d*), an inclusion, figure 6 (*b*), is reconstructed with {1 1 0} facets. Small {2 1 1} facets appear along some edges.

It is difficult to discriminate whether the inclusions correspond to 'positive' crystals (cubic inclusions surrounded by the isotropic liquid) or to 'negative' crystals (inclusions of isotropic liquid surrounded by the cubic phase). Inclusions in different parts of the observation field have the same orientation, which suggests that they are negative crystals [13]. On the other hand, their sizes increase with decreasing temperature, as would be the case for cubic inclusions (positive crystals). Nevertheless, in both cases, facets develop at the same cubic/isotropic liquid interface.

3.3.3. *A free drop deposited on a treated (hydrophobic) glass plate*

Small free drops deposited on the treated surface were first heated to 182°C. This is well above the transition line indicated in the phase diagram (172°C). This phenomenon of retarded fusion is known in similar liquid crystalline systems (thermotropic cubic phases [11], TGB phases [19] and blue phases [20]). It has been interpreted in some cases as due to a two-stage process: some local order reminiscent of that in the cubic phase may persist above the destruction of the long range order.

The droplets were then cooled slowly (0.2°C min^{-1}) into the biphasic region (154°C). The coexistence of facetted cubic crystals and isotropic liquid shows clearly, figure 7 (*a*). On further cooling and annealing the system at 138°C, cubic germs grow and become more sharply facetted, figure 7 (*b*). The droplets shown in the pictures

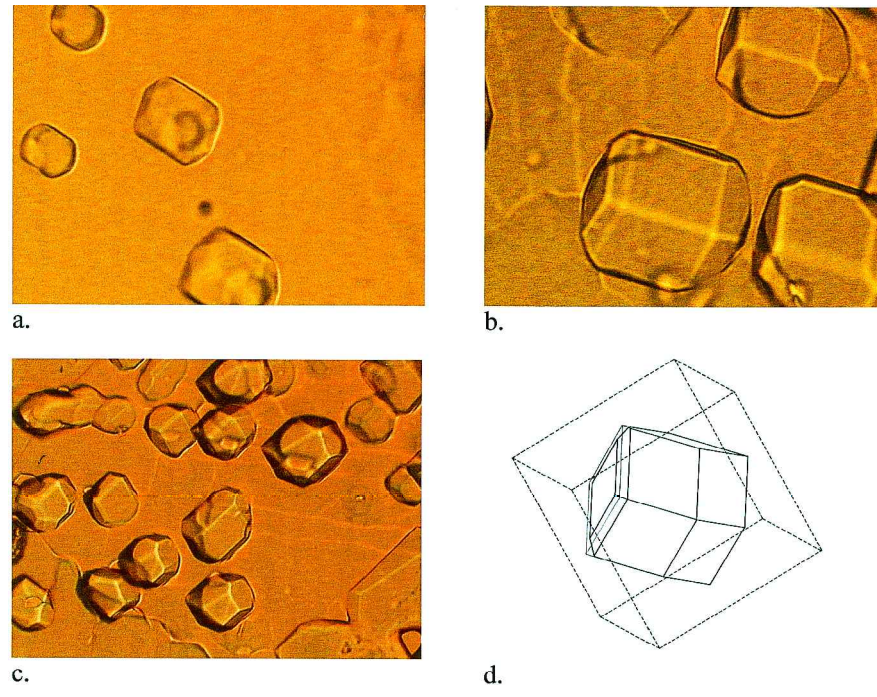

Figure 6. Coexistence of the liquid isotropic phase and the $Im\bar{3}m$ cubic phase in the mixture, observed in a free drop. (*a*) Quasi-spherical inclusions at the beginning of the facetting process; (*b*), (*c*) completely facetted inclusions observed along different directions; (*d*) polyhedron constructed with (1 1 0) planes, to be compared with (*b*), small (2 1 1) facets along some edges reproduce the pattern shown in (*b*).

Downloaded At: 18:27 25 January 2011

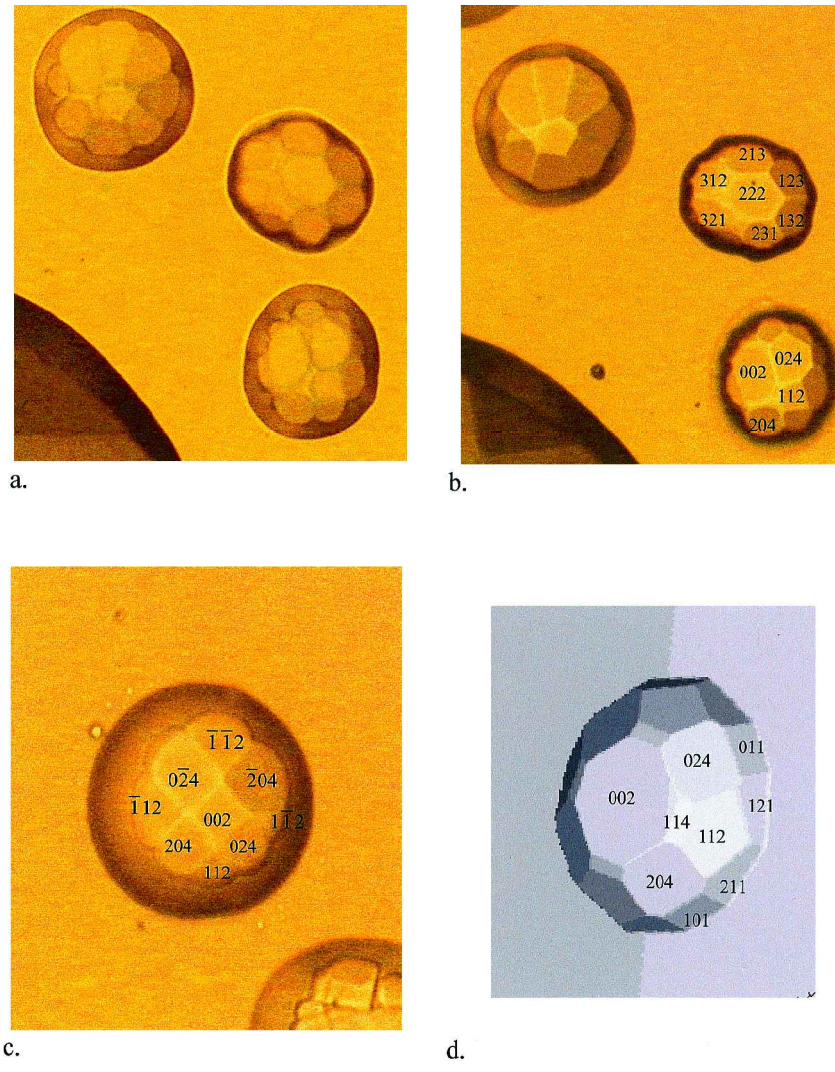

Figure 7. Coexistence of the isotropic phase and the $Im\bar{3}m$ cubic phase in the mixture, observed in small free drops on treated glass. (*a*) Droplets at 154°C, facetted $Im\bar{3}m$ cubic crystals in the centre, isotropic phase at the periphery; Symmetrical patterns with 3-fold symmetry (middle) and 2-fold symmetry (mirror plane) (bottom). (*b*) The same preparation as in (*a*), annealed at 138°C during one night; (*c*) another droplet in the same preparation as in (*a*), at 152°C, showing a 4-fold symmetric pattern; (*d*) a tentative reconstruction of the facetting of the drop in (*b*) (bottom).

Downloaded At: 18:27 25 January 2011

correspond to single crystals viewed in different orientations. In figure 7 (*c*), a 4-fold axis, i.e. a [0 0 1] direction, is almost perpendicular to the surface. Then, the square facet perpendicular to this axis corresponds to a (0 0 2) reticular plane (due to the $Im\bar{3}m$ space group, the inter-reticular spacing in this direction is d_{002}). This facet is surrounded by two kinds of facets, according to the 4-fold symmetry. The first kind of neighbouring facets are adjacent by an edge to the central one and are of the type $(q, 0, p)$ (with p and q integers)—they may correspond for example to the four reticular plane families (2 0 4), (0 2 4), $(\bar{2}\,0\,4)$ and $(0\,\bar{2}\,4)$. The second kind, adjacent by a vertex, are of the type (q, q, p)—corresponding for example to the families (1 1 2), $(\bar{1}\,1\,2)$, $(\bar{1}\,\bar{1}\,2)$ and $(1\,\bar{1}\,2)$. In the drop in the middle of figure 7 (*b*), a 3-fold axis is perpendicular to the surface. The hexagonal facet corresponds to a (2 2 2) reticular plane. Surrounding facets are placed according to an apparent 6-fold symmetry. They have indices of the general form $(p - q, p, p + q)$ (with p and q integers and $p > q$) and may correspond for example to the 6 families (1 2 3) (with all permutations of the indices). It is interesting to note that the 3 2 1 reflection is an intense one in the diffraction pattern (see the table). The drop at the bottom of figure 7 (*b*) also exhibits a highly symmetric pattern. However, it does not have a simple orientation. A mirror plane is roughly orthogonal to the substrate surface. In figure 7 (*d*) we present a portion of a crystal which tentatively reproduces this drop. This reconstructed crystal is built by selecting an ensemble of planes belonging to the $Im\bar{3}m$ space group and placing them at similar (but not identical) distances from the origin, so as to reproduce qualitatively the shape observed in figure 7 (*b*). Specifically, all the angles between edges are reproduced. Note that the {0 0 4} (equivalent to {0 0 2} from the facetting point of view) and {4 1 1} facets correspond to intense Bragg peaks (see the table). However, an exact determination of

the Miller indices of all facets shown on the crystals in figure 7 would require measurement of the angles between facets, or, equivalently, the average curvature of the drops. This is postponed to future work.

4. Discussion

Liquid crystals are one of the very few systems in which it may be possible to observe easily equilibrium crystal shapes [21]. We have observed facetted single crystals in both $Ia\bar{3}d$ and $Im\bar{3}m$ cubic phases. We will now discuss the origin of the facetting process, in the case of equilibrium or growth shapes.

On facetted crystals at equilibrium, facets correspond to surfaces or interfaces with the lowest surface energy [22, 23]. As a general rule in crystals, these facets are related to the most dense reticular planes or cleaving planes. On the other hand, the most dense reticular planes have the largest inter-reticular spacing and thus give rise to the first Bragg reflections (i.e. Bragg peaks at the smallest q vectors) in diffraction experiments. Therefore, there should be a direct relationship between equilibrium facetting and crystallographic structure.

Downloaded At: 18:27 25 January 2011

However, even in perfectly controlled conditions, equilibrium crystal shapes are difficult to observe for intrinsic reasons. Observed shapes generally results from fast or slow growth and surface reorganization processes. Specifically, rough surfaces have a much faster growth rate than facetted ones, because such surfaces (or interfaces) may grow continuously, whereas growing a macroscopic facet requires nucleating a new reticular plane, which requires a nucleation barrier large compared to kT. Most developed facets are those with the slowest growing rates, which means those with the highest nucleation barriers, which are not necessarily those with the lowest surface energy at equilibrium. Non-equilibrium (growing) shapes are often *more* facetted than equilibrium ones. However, it may be supposed that the larger the inter-reticular distance in a $[h\,k\,l]$ direction, the higher the nucleation barrier of the corresponding facets. It is therefore justifiable to discuss the relationship between the observed growing shapes and the crystallographic data in the observed phases.

Most crystal shapes observed here are certainly not at equilibrium, for several reasons. First, the time scale of the observations is probably not long enough to allow equilibration. It has been observed that crystals with different shapes may coexist for several hours or days in the same preparation, which proves that these shapes are determined by the growth conditions. Second, the temperature should be perfectly homogeneous; here, it is perhaps somewhat lower at the surface of the drops than close to the substrate. Lastly, impurities may come from the degradation of the compounds themselves upon heating at a relatively high temperature for several hours. Even at small fractions of impurities, these may segregate at the surfaces or interfaces of the crystals, thus modifying the thermodynamic properties of the surfaces/interfaces significantly. Note that care was taken to use glass plates treated with *grafted* silane chains, in order to avoid the eventual contamination of the preparation by a deposited surface treatment agent.

Nevertheless, it may be tempting to consider the crystals in figure 6 as close to equilibrium shapes (as was done in [13]). In this case, the temperature has been decreased extremely slowly ($0.1°\,h^{-1}$). Germs first appear as non-facetted and rather irregularly shaped. Germ sizes have been stabilized for about one day. Facets develop during this time, leading to very regular polyhedral shapes. Moreover, germs with different sizes have the same homothetic shape.

All the observations in § 3.2. (figures 3 and 4) suggest that the (2 2 0) reticular planes play a predominant role in the surface properties at the air/cubic interface of the $Ia\bar{3}d$ cubic phase obtained for the pure compound. This is in contrast to the $Ia\bar{3}d$ cubic phase observed in $C_{12}EO_6/H_2O$ and in other lyotropic systems, in which (2 1 1) planes are known to appear most frequently at free surfaces or as cleaving planes [13, 24]. The (2 2 0) reticular planes, however, correspond to the second most intense Bragg peak in the structure of this phase, in the order of growing reticular distance. Indeed, due to the extinction rules of the $Ia\bar{3}d$ space group ($h\,k\,l$: $h+k+l=2n$; $h\,k\,0$: $h,k=2n$; $h\,h\,l$: $2h+l=4n$; $h\,0\,0$: $h=4n$), there are two well separated Bragg peaks corresponding to large inter-reticular spacings, which are 2 1 1 and 2 2 0 (see the table).

The case of the $Im\bar{3}m$ phase is more puzzling. Due to the higher symmetry of this phase, the only extinction rule is: $h\,k\,l$: $h+k+l=2n$. A very peculiar repartition of the intensity of the reflections, characteristic of $Im\bar{3}m$ cubic phases [9], is observed on a powder diagram. Bragg reflections corresponding to the largest d_{hkl} values have very weak or even unobservable intensities (see the table). In this case, the first intense reflections (3 2 1, 4 0 0, 4 1 1, 3 3 0) have to be considered to predict the cleaving planes. These reflections have quite comparable inter-reticular spacings (see the table) and one could expect that all the corresponding facets might be observed.

This is in accordance with the observation of the single crystals at the air/cubic interface (figure 7). Small drops of the mixture, deposited on a hydrophobically treated glass plate, often lead to the growth of single crystals under conditions of slow growth. Depending on the crystal orientation with respect to the surface of the substrate, a number of different facets appear. All of them correspond to reticular planes with large inter-reticular distances which give allowed Bragg reflections. However, a detailed study of the crystal shapes in figure 7

would require the relative orientations of facets to be measured. Specifically, the average contact angle with the substrate should be measured.

The observations involving coexistence with the liquid isotropic phase (figure 6) show that the (1 1 0) reticular planes are predominant. This fact seems difficult to relate to the X-ray data. To do this, we should investigate more carefully the relative intensities of the reflections along the [1 1 0] direction (1 1 0, 2 2 0, 3 3 0 and 4 4 0) by using single crystal analysis, because the 3 3 0 and 4 1 1 reflections are superimposed on a powder diagram. This would determine which inter-reticular distance (d_{110}, d_{220}, d_{330} or d_{440}) is really involved in the facetting process. Moreover, this could help us to understand better the structure of the $Im\bar{3}m$ cubic phase.

5. Conclusion

The systems studied exhibit two different cubic phases, according to the relative fraction of compound **2**. We have studied the growth of both cubic phases, either in the fluid isotropic or smectic C phases, under different growing conditions. It is shown that rather large (50 μm) single crystals may be obtained easily and observed by optical microscopy. The facetting of these crystals is described at the interface with air or with the liquid isotropic phase. The observed crystal habits are growth shapes, rather than equilibrium shapes. It is shown that it is difficult at this stage to use the observed crystal shapes to discriminate unambiguously the different cubic phases. In the pure compound ($Ia\bar{3}d$ cubic space group), the facets at the air/cubic interface are interpreted with (2 2 0) reticular planes. In the mixture ($Im\bar{3}m$ cubic space group), between glass plates, the facets at the isotropic liquid/cubic interface are interpreted with (2 0 0), (1 1 0) and (2 2 2) planes; in free drops, highly symmetric shapes, which correspond to the polyhedron constructed with (1 1 0) planes, are observed. Monocrystals of the $Im\bar{3}m$ cubic phase are observed on treated glass plates. They exhibit a variety of facets, which belong to the $Im\bar{3}m$ space group.

We wish to thank H. Delacroix, A. M. Levelut and P. Pieranski for stimulating discussions.

References

[1] Mariani, P., Luzzati, V., and Delacroix, H., 1988, *J. mol. Biol.*, **204,** 165.
[2] Fontell, K., 1990, *Colloid polym. Sci.*, **268,** 264.
[3] Charvolin, J., and Sadoc, J. F., 1987, *J. Phys. Fr.*, **48,** 1559.
[4] Clerc, M., and Dubois-Violette, E., 1994, *J. Phys. II Fr.*, **4,** 275.
[5] Clerc, M., Hendrikx, Y., and Farago, B., 1997, *J. Phys. II Fr.*, **7,** 1205.
[6] Gray, G. W., Jones, B., and Marson, F., 1957, *J. chem. Soc.*, 393.
[7] Kutsumizu, S., Yamada, M., and Yano, S., 1994, *Liq. Cryst.*, **16,** 1109.
[8] Tardieu, A., and Billard, J., 1976, *J. Phys. Coll.*, **37,** C-3.
[9] Levelut, A. M., and Clerc, M., 1998, *Liq. Cryst.*, **24,** 105.
[10] Kutsumizu, S., Ichikawa, T., Nojima, S., and Yano, S., 1999, *Chem. Commun.*, 1181.
[11] Saito, K., Sato, A., and Sorai, M., 1998, *Liq. Cryst.*, **25,** 525.
[12] Barbet-Massin, R., Cladis, P. E., and Pieranski, P., 1984, *Phys. Rev. A*, **30,** 1161.
[13] Sotta, P., 1991, *J. Phys. II Fr.*, **1,** 763.
[14] Pieranski, P., Sotta, P., Rohe, D., and Imperor-Clerc, M., 2000, *Phys. Rev. Lett.*, **84,** 2409.
[15] Gray, G. W., Hartley, J. B., and Jones, B., 1955, *J. chem. Soc.*, 1412.
[16] Strzelecka, H., Jallabert, C., Veber, M., and Malthete, J., 1988, *Mol. Cryst. liq. Cryst.*, **156,** 347.
[17] Kahn, F. J., 1973, *Appl. Phys. Lett.*, **22,** 386.
[18] Levelut, A. M., private communication.
[19] Goodby, J. W., Nishiyama, I., Slaney, A. J., Booth, C. J., and Toyne, K. J., 1993, *Liq. Cryst.*, **14,** 37.
[20] Goodby, J. W., Dunmur, D. A., and Collings, P. J., 1995, *Liq. Cryst.*, **19,** 703.
[21] Geminard, J. C., and Oswald, P., 1997, *Phys. Rev. E*, **55,** 4442.
[22] Wortis, M., 1988, in *Chemistry and Physics of Solid Surfaces*, Vol. VII, edited by R. Vanselow (Berlin: Springer Verlag).
[23] Kern, R., 1987, *Morphology of Crystal A*, edited by I. Sunagawa (Dordrecht: Reidel).
[24] Delacroix, H., Mariani, P., and Gulik-Krzywicki, T., 1990, *J. Phys. Colloq. Fr.*, C7-119.

Downloaded At: 18:27 25 January 2011